Monitoring of tension force and load transfer of ground anchor by using optical FBG sensors embedded tendon

Young-Sang Kim[1], Hyun-Jong sung[2], Hyun-Woo Kim[2] and Jae-Min Kim*

Department of Marine & Civil Engineering, Chonnam National University, Yeosu 550-749, Korea

(Received July 3, 2010, Accepted November 4, 2010)

Abstract.   A specially designed tendon, which is proposed by embedding an FBG sensor into the center king cable of a 7-wire strand tendon, was applied to monitor the prestress force and load transfer of ground anchor. A series of tensile tests and a model pullout test were performed to verify the feasibility of the proposed smart tendon as a measuring sensor of tension force and load transfer along the tendon. The smart tendon has proven to be very effective for monitoring prestress force and load transfer by measuring the strain change of the tendon at the free part and the fixed part of ground anchor, respectively. Two 11.5 m long proto-type ground anchors were made simply by replacing a tendon with the proposed smart tendon and prestress forces of each anchor were monitored during the loading-unloading step using both FBG sensor embedded in the smart tendon and the conventional load cell. By comparing the prestress forces measured by the smart tendon and load cell, it was found that the prestress force monitored from the FBG sensor located at the free part is comparable to that measured from the conventional load cell. Furthermore, the load transfer of prestressing force at the tendon-grout interface was clearly measured from the FBGs distributed along the fixed part. From these pullout tests, the proposed smart tendon is not only expected to be an alternative monitoring tool for measuring prestress force from the introducing stage to the long-term period for health monitoring of the ground anchor but also can be used to improve design practice through determining the economic fixed length by practically measuring the load transfer depth.

Keywords: ground anchor; prestressing force; load transfer; Fiber Bragg Grating (FBG); smart tendon; pullout test.

1. Introduction

Despite the increasing popularity of the 7-wire strand tendon for a cable-stayed bridge and geo-reinforcement system such as a rock or soil anchor, no accurate or simple method is available for directly measuring the prestress force of these systems. The measurement of introduced prestress force is important for monitoring excessive wind or traffic loading, failure foreboding of retaining wall or soil slope, gauging the redistribution forces present after a seismic event, and detecting corrosion via loss of the cross section on both the geo-reinforcement system and the cable-stayed bridge system.

Following the sudden collapse of the Ynys-y-Gwas bridge in 1985 and the Malle bridge in 1992, many post-tensioned concrete bridges were inspected (Fricker and Vogel 2006). As a result, it was

---
*Corresponding Author, Professor, E-mail: jm4kim@chonnam.ac.kr
[1]Associate professor, Ph.D.
[2]Graduate student

realized that the post-tension system is subject to long-term risk such as corrosion of the tendon caused by ingress of water and chloride irons into partially grouted ducts (Youn and Kim 2006, Bruce 2008). The tension of a prestressing strand can vary due to the variety of losses including (1) instantaneous losses such as elastic shortening, friction, and anchorage set occurring at the time of the transfer of the prestressing force, and (2) time dependent losses due to steel relaxation, concrete creep, shrinkage and sudden displacement of fixed ground that occur after transfer and during the life of the member. Accordingly, the measurement of tensile force of the tendon becomes very important for long-term maintenance of the ground anchor as well as the bridge's design purpose (Brady and Bush 2001, Moerman *et al.* 2005, Shenoy and Frantz 1991, Aalami 1998, Lakshmanan *et al*. 2009, Anastasis *et al.* 2005, Wang 2008).

Various attempts have been made to estimate the tension force in the field by attaching sensors such as Tensmeg (http://www.rstinstruments.com) directly onto the outside of the tendon, or indirectly by sensing the strain near the tendon using the electrical strain gauge and vibrating wire strain gauge (VWSG) installed in concrete or on a rebar near the duct (Onyemelukwe and Kunnath 1997, Pantelides *et al.* 2007). Typically, center-hole load cells have also been used to measure load in ground anchors. The load-bearing element is a cylinder of high strength stainless steel. Multiple strain gauge rosettes are bonded to the cylinder and are evenly spaced around the periphery. Through proper calibration, these strain readings can be correlated to the force applied to the load cell (Moerman *et al.* 2005). However, these kinds of electromechanical sensors are also subject to long-term risk as well as suffering from noise during long distance transmission and immunity to electromagnetic interference (EMI).

On the other hand, unlike the conventional electromechanical sensors, fiber optic sensors (FOSs) have, for a long time now, proven to be a reliable sensing element for the measurement of various physical, chemical, and biological parameters (Udd 1995). Among the FOSs, Fiber Bragg Grating (FBG) is particularly useful in monitoring civil infra-structures because the inherent self-referencing capability of the FBG, which is not affected by fluctuations in the light source intensity, makes possible a high degree of serial multiplexing along the length of a fiber (Vurpillot *et al.* 1996, Meissner *et al.* 1997, Inaudi 2000, Lau 2003, Calvert and Mooney 2004, Li *et al*. 2005, Nellen *et al*. 1999(a,b), Ren *et al.* 2005, Kim *et al.* 2009, Talebinejad *et al.* 2009, Kesavan *et al.* 2005). However, for a successful field application of the optical sensor to a harsh environment of construction, a proper encapsulation technique needs to be developed for each application (Zhou *et al.* 2003).

In this study, a ground anchor was developed which has FBG sensor embedded smart tendon to monitor the introduced prestress force as well as load transfer phenomenon and was tested in various manners to show the feasibility of the proposed system. A series of laboratory tests was performed to verify the feasibility of the FBG sensor as a measuring sensor of strain along the tendon. Prototype anchors were made by using FBG sensor embedded smart tendons and installed into the ground conditions. Tension forces of each loading-unloading step and load transfer along the anchor were monitored using FBG sensors. Prestress forces determined by using the smart tendon were compared with those measured from a conventional load cell.

2. FBG sensor embedded tendon – smart tendon

2.1 FBG sensor

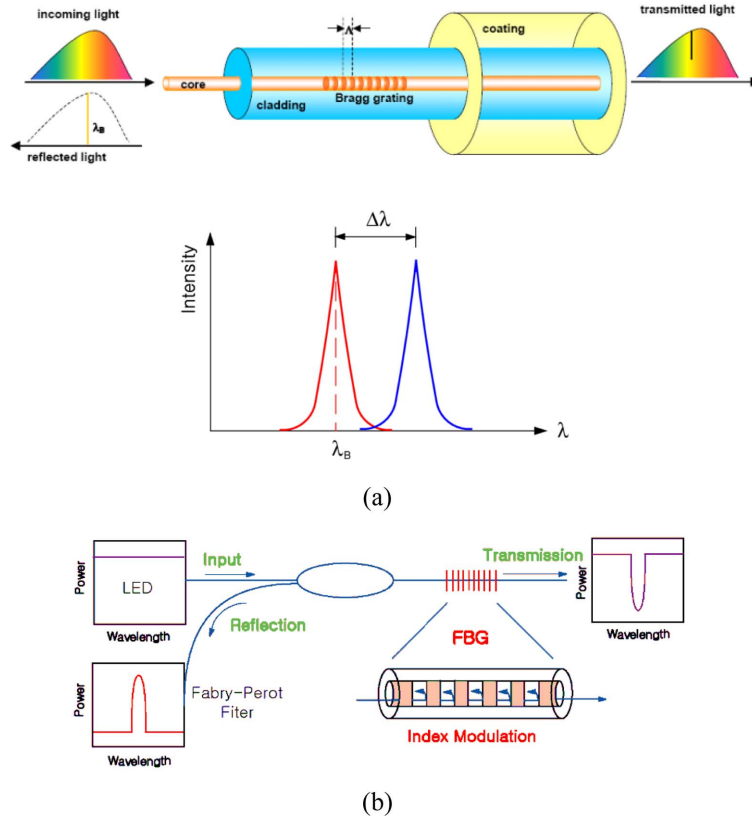Fiber Bragg grating is a modulated refractive index scribed by ultraviolet (UV) light with a

Fig. 1 Fundamentals of FBG sensor and measurement setup: (a) fundamentals of FBG sensor, (b) schematic diagram of measurement setup

periodic spacing as shown in Fig. 1. It is widely used as sensor elements, suitable for measuring static and dynamic fields such as strain and temperature, because of its high sensitivity, linearity in response over many orders of magnitude, immunity to EMI, high temperature tolerance, and serial multiplexing capability and so on (Othonos and Kalli 1999). Fig. 1 depicts the fundamental properties of the FBG sensor and the typical measurement setup including the interrogator. In general, the length of the FBG sensor is less than 2.0 cm.

When a light source with a broadband wavelength spectrum is inflicted into the optical fiber, the Bragg grating reflects light waves with a narrowband spectrum (Fig. 1(a)). This allows us to obtain a reflection spectrum that is only dependent on the amount of changes at the grated region. The center wavelength of the reflected light, λ_B, varies with the refractive index of the optical fiber, n_{eff}, and the spacing between the grating planes, Λ, as follows

$$\lambda_B = 2n_{eff}\Lambda \tag{1}$$

The center wavelength ranges typically from 1510 nm to 1590 nm.

Both the index of refraction and the pitch length of the spacing are independently affected by changes in strain and temperature. Thus the shift in center wavelength of the *BG*, $\Delta\lambda_B$, induced by strain and temperature changes, respectively $\Delta\varepsilon$ and ΔT, is given by (Othonos and Kalli 1999)

$$\frac{\Delta\lambda_B}{\lambda_B} = (1 - P_e)\Delta\varepsilon + (\alpha + \xi)\Delta T \tag{2}$$

where p_e is an effective strain-optic constant (approximately 0.22 for silica), α is the thermal expansion coefficient of the fiber (approximately 0.55×10^{-6} for silica), and ξ represents the thermo-optic coefficient (approximately 8.6×10^{-6} for germania-doped silica-core fiber). It should be noted that the change in strain in Eq. (2) is purely a result of external actions excluding temperature change since the thermal strain is considered in the second term. From Eq. (2) the strain change can easily be computed based on the shift of center wavelength in the spectrum of a reflected light wave, if the temperature is known. Under the simultaneous perturbations of strain and temperature, a measurement technique utilizing two FBG sensors with different gratings can be employed, provided that two linear equations of Eq. (2) obtained from two different FBG sensors can be solved (Othonos and Kalli 1999). However, since the temperature change ΔT in Eq. (2) may be small enough to be neglected under the ground, Eq. (2) can be rearranged into the following Eq. (3) and strain change can be easily calculated from the change of reflected wavelength.

$$\Delta\varepsilon = \frac{1}{(1 - P_e)}\frac{\Delta\lambda_B}{\lambda_B} \tag{3}$$

2.2 Encapsulation of FBG into 7-wire steel tendon

In this study, an encapsulation method of optical fiber with BG sensors into a 7-wire strand is applied as shown in Fig. 2. This takes advantage of the fact that a central steel wire of the 7-wire strand called 'king wire' is straight, while the other six wires wrap the king wire helically. In order to encapsulate the FBG sensor into the tendon, we developed the idea of replacing the king wire with a steel tube in which the optical fiber including FBG sensors is embedded. Since the diameter of a typical optical fiber is approximately 1/4 mm, a steel tube with an inside diameter of 2.0 mm or less is large enough to accommodate the fiber and liquid glue such as epoxy resin with low viscosity. Fig. 3 shows a cross section of the tendon including a tube with a diameter of 5.24 mm and an inside diameter of 1.0~2.0 mm.
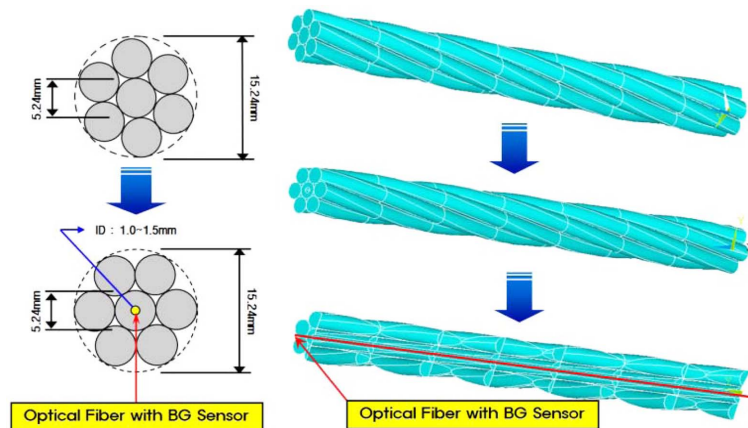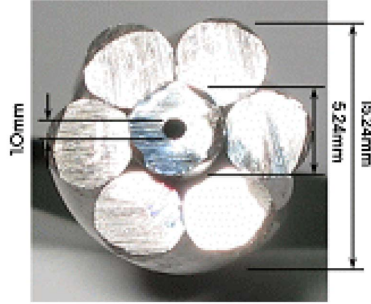

Fig. 2 Concept of smart tendon

Fig. 3 A cross-section of real smart tendon

The steel tube can easily be manufactured by the pultrusion process. The manufacturer working on the project is currently capable of extending its length up to 34.0 m, and the inside diameter of the steel tube ranges from 1.0 mm to 2.0 mm. The tube is usually made of mild steel for an easier pultrusion process, and then it is heat-treated to draw level with a higher tensile strength of prestressing tendon. Currently, the yield strength of the tube is typically 50% of the wire in the prestressing tendon, while that of the mild steel is approximately 1/3 of the high-strength wire. We are expecting that the strength of the tube can be further improved in the near future.

We constructed several smart tendon specimens of 1.0 m long with one FBG sensor, and carried out a tensile load test using UTM as shown in Fig. 4. The strain gauge is attached on the outside helical wire of the tendon for comparison, and the load applied includes loading-unloading sequences up to 50 kN as shown in Fig. 5.

The axial strain in the longitudinal direction of the tendon, ε_{xx}, can be obtained from the strain measured on the inclined helical wire, $\varepsilon_{\beta\beta}$, depending on the angle of the helical wire from the axis denoted as β, as follows

$$\varepsilon_{xx} = \frac{1}{\cos^2\beta}\varepsilon_{\beta\beta} \tag{4}$$
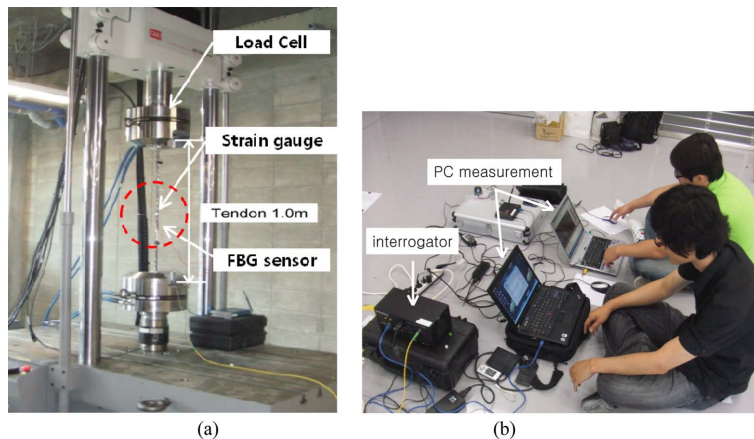

(a)   (b)

Fig. 4 Test setup of 1.0 m long smart tendon FBG specimen: (a) specimen mounted on UTM, (b) data acquisition system
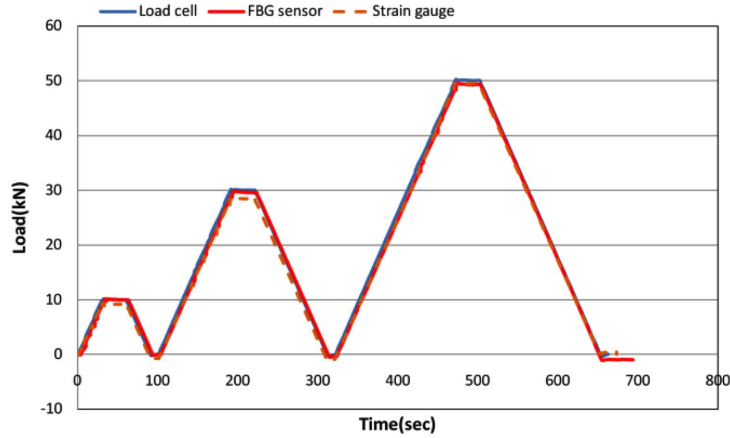
Fig. 5 Tensile test results of 1.0 m long in-tendon FBG specimen

The tensile forces of the tendon were estimated by multiplying measured strains, the effective cross-sectional area of the tendon (A_t = 140 mm^2), and Young's modulus of the tendon (E_t = 200 GPa). The strain measurements compared in Fig. 5 indicate that the tensile forces estimated using the proposed smart tendon are almost identical to the loads inflicted on the tendon. From the test results for the 1.0 m long smart tendon specimen, we could conclude that proposed smart tendon system is viable for measuring the prestress force of a 7-wire strand.

3. Applications to ground anchor monitoring

3.1 Monitoring of load transfer of 1m-length model anchor

For the ground anchor, it is important to monitor not only the prestress tension force but also the load transfer and stress distribution along the anchor according to the introduction of prestress load. To this end, a model pullout test was carried out to monitor the load transfer phenomenon and distribution of shear stress around the tendon using a proposed smart tendon.

After manufacturing the 1.0 m long smart tendon, in which 5 FBG sensors are located at different positions as shown in Fig. 6, the tendon was fixed to the model rock body with grout to model the installation conditions of the ground anchor. Fig. 6 shows the location and initial reflection wavelength of FBGs and a photograph of the pullout test setup of the model anchor. Interrogator of Welltech co. Ltd was used to monitor the change of reflected wavelength due to strain change.

A static pullout test was carried out by following the BS 8081 code for the anchor pullout test. With an initial pullout load of 4.9 kN, 7 loading steps - e.g., 19.6, 29.4, 39.2, 49.0, 58.8, 78.5, 98.1 kN - were applied up to 98.1 kN maximum load as shown in Fig. 7. Bonding failure between the grout and model rock occurred at 90.2 kN as shown at Fig. 7. During the increase of the applied load, the elongation of the tendon and the grout movement were measured by LVDT.

Fig. 8(a) shows the strains measured from 5 FBG sensors with respect to loading time. As shown in the figure, FBGs located at 5 cm and 15 cm detect the strain changes from the beginning of the loading step. However, FBG located at a 65 cm depth detects no strain almost up to a 39.2 kN loading step. As can be seen more clearly at the strain-depth relationship of Fig. 8(b), only the FBG
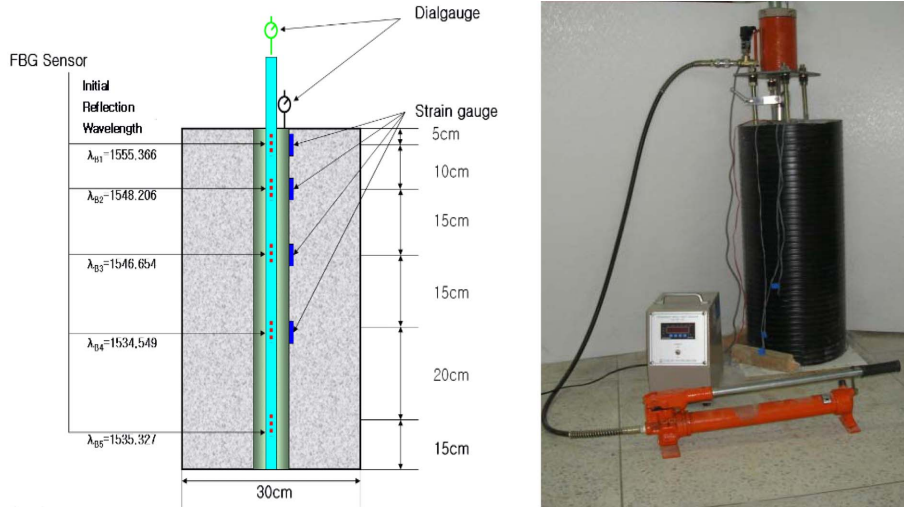
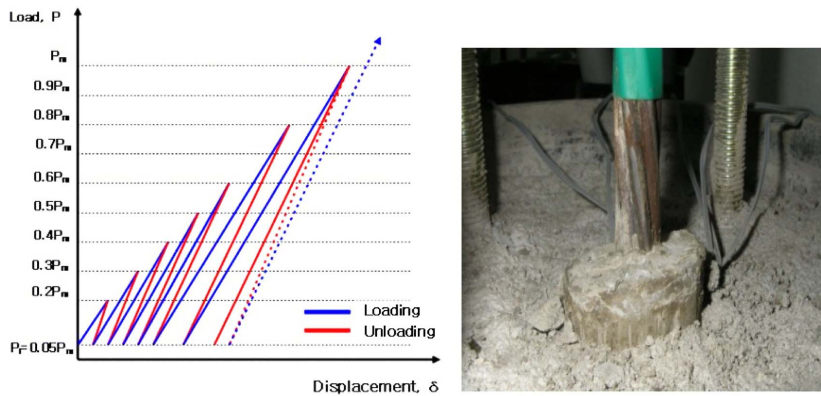Fig. 6 Locations and initial reflection wavelength of FBGs and pullout test setup of model anchor

Fig. 7 Loading steps of pullout test and photograph taken after the end of pullout test

sensor at a 5 cm depth detects strain, even at 4.9 kN, but no strains occur at other FBG sensors. However, the strain at each FBG sensor increases with respect to the load increase inflicted at the anchor head by the oil pressure pump and jack. As can be shown in Fig. 8(b), the distribution shape of the strain at each loading step is not constant, but is highly non-linear, as pointed by other researchers (Aydan *et al.* 1993. 1995, Farmer 1975, Won *et al.* 2001). This means that stresses of only the upper part of the tendon-grout-rock interfaces were mobilized to resist the applied load at a small loading step. However, stresses over the larger area of interfaces were mobilized with respect to load increase. This means that the applied prestress force was transferred from the upper part of the anchor interface to the lower part of the anchor to resist the large prestress force. The right hand side of Fig. 8(b) shows the strain measurement of a conventional electromagnetic strain gauge attached at the surface of the grout-rock interface. Originally, 4 strain gauges were attached with FBGs at the same positions. However, the strain gauge at 40 cm depth was damaged during specimen preparation and only 3 strain gauges were active to measure the strain change at the grout-rock interface. Strain measurements from the conventional strain gauges also illustrate the progressive failure by load

(a) Time-mobilized strain from FBGs

(b) Load transfer and strain redistribution along the tendon
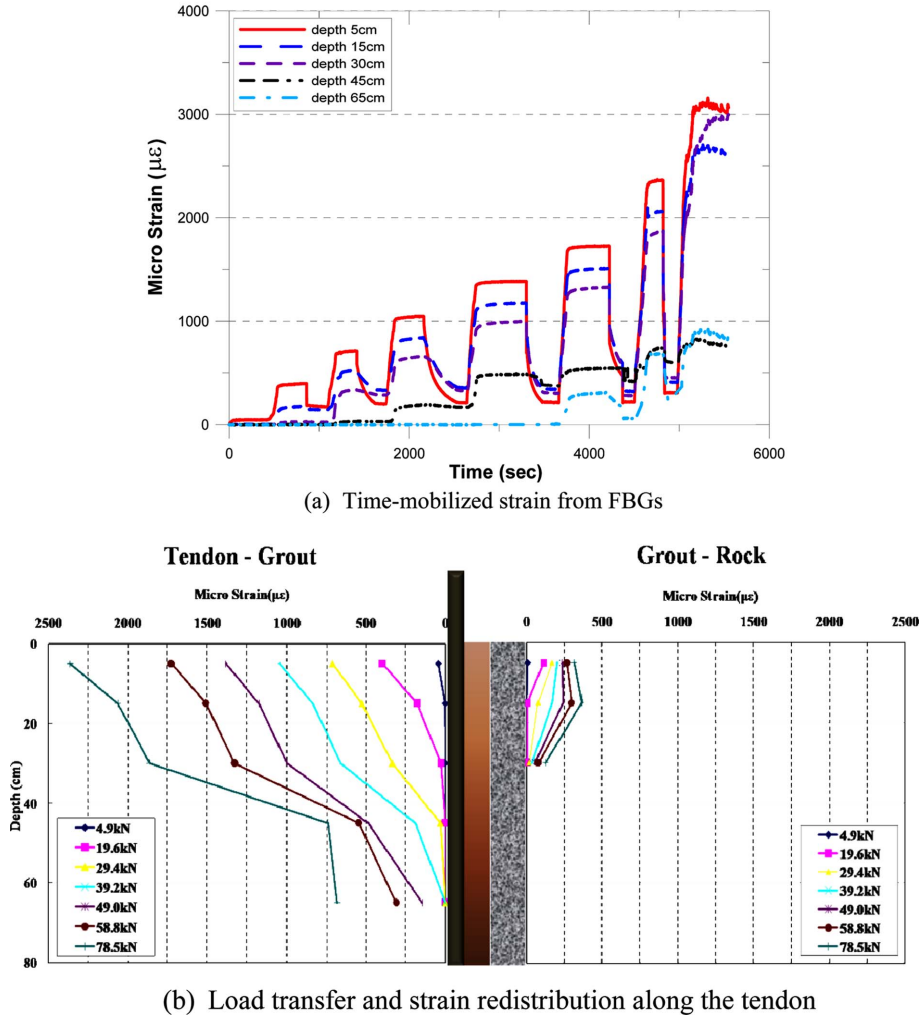
Fig. 8 Strain measurements results from the pullout test: (a) time-strain curves measured at each FBG sensor, (b) distribution of strain at the tendon-grout-rock interface w.r.t. load increase

transfer phenomenon between the grout and rock body (Won *et al.* 2001).

Shear stress at the interface of the tendon and grout can be determined based on the measured strains using FBG sensors as follows. Fig. 9 shows the determined shear stress distributions with the theoretical shear stress distributions based on Farmer (1975) and Aydan *et al*. (1993, 1995).

$$\tau_{tg} = \frac{E_t \cdot \gamma_t}{2d} d\varepsilon \qquad (5)$$

where τ_{tg} is an average shear stress between two stress calculation points, d is a distance between two points, E_t is an elastic modulus of tendon, $d\varepsilon$ is a difference of strain measured from two points. The difference of strain between two points can be estimated from the continuous function, which is determined from the regression analysis of the measured strain using FBG sensors of smart tendon.

From Figs. 9(a) and 9(b), it can be seen that not only shear stress τ_{tg} which is calculated based on
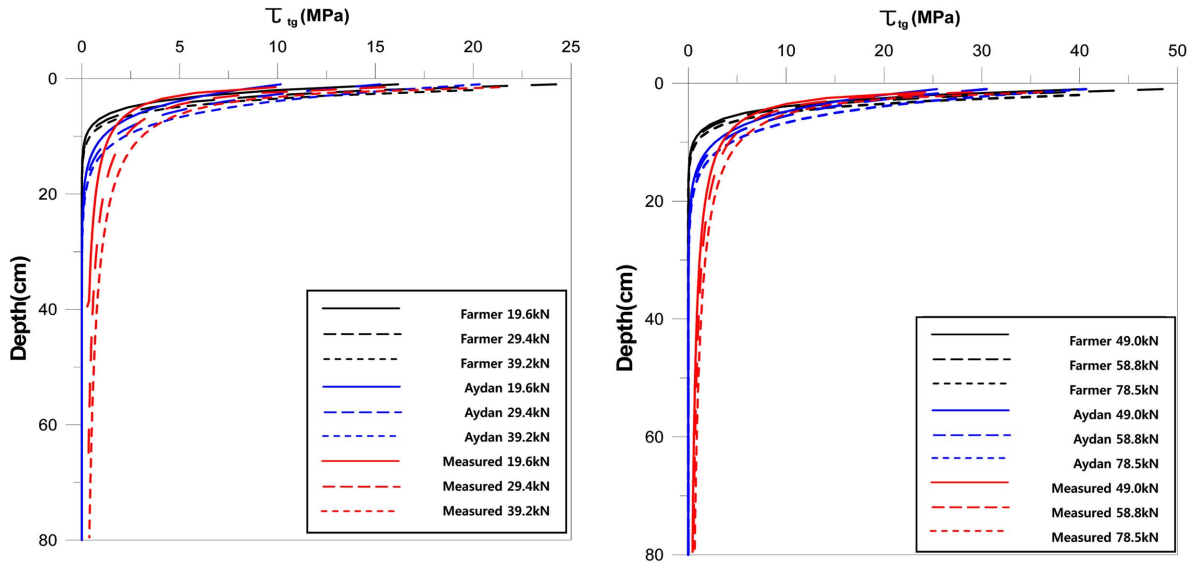
Fig. 9 Shear stress distributions determined from strain measurement of FBGs and analytical solutions

the measured strains using FBGs increases with increase of introduced prestress force but also load transfer depth increases with load increase. On the other hand, theoretical solutions developed by Aydan *et al.* and Farmer underestimate the load transfer depth and magnitude of shear stresses mobilized at the interface of the tendon and grout. From the pullout test result, the smart tendon can successfully show the load transfer phenomenon by measuring the strain change of the 7 wire strand very effectively until the end of the tensile failure of the grout body. It is expected that a new empirical relationship can be developed from the pullout test results using the proposed smart tendon to make present design of anchor economically.

3.2 Monitoring of proto-type ground anchor

A challenging research project for the field application of the smart tendon was planned. Two 11.5 m long proto-type anchors were manufactured, as shown in Fig. 10, at the factory of Sam Woo Geotechnical Co. Ltd, which is a major company in the production of anchors in Korea. The dimensions and design conditions of these anchors are summarized in Table 1. The two anchors have the same dimensions but a different fixed length, which is usually a length used in geotechnical practice. They were installed at the construction site of ECCHE (Experimental Center for Costal and Harbor Engineering) in Chonnam National University of Korea as shown in Fig. 12.

Five FBG sensors are allocated at each tendon as shown in Fig. 11. Since the first FBG sensor is located at free part, where the tendon is not fixed to the surrounding ground, the strain measured at the first FBG sensor can be used to estimate the prestress force directly. Since the other FBG sensors are located at a fixed part, where tendons are fixed to the soil or rock with grout, strains measured from those FBGs can be used to estimate the load transfer between the tendon and grout.

Prestress forces are introduced by using an oil pressure pump and jack as shown in Fig. 12, and for comparison, the introduced prestress force was carefully measured by both conventional load cell and proposed smart tendon. Fig. 13 shows the result of wavelength shift measured from the
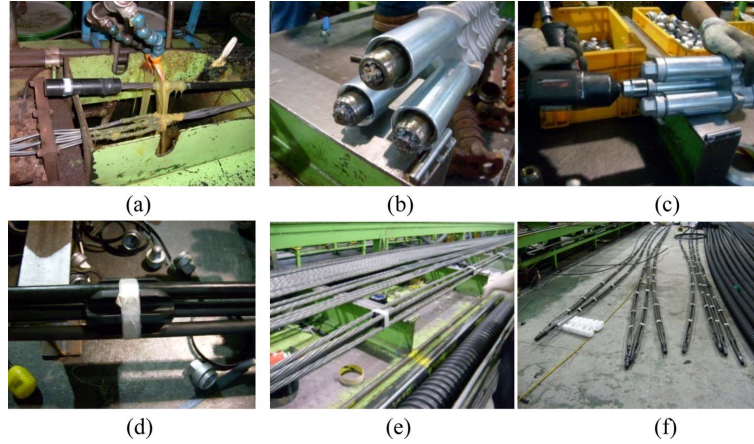
Fig. 10 Manufacturing process of prototype anchor (SamWoo Geotechnical Co. Ltd): (a) Sheath tube insertion, (b) end plate insertion, (c) end plate fixing, (d) spacer fixing, (e) anchor assembly, (f) end product - anchor

Table 1 Dimensions of proto-type anchor and design condition of anchor for the pullout test

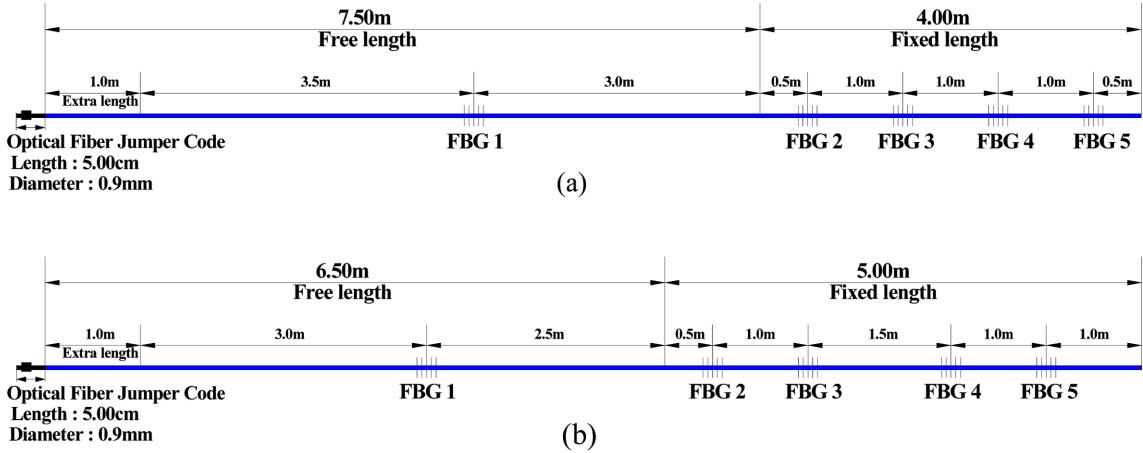| No.	Anchor length (m)	Free length (m)	Fixed length (m)	Boring depth (m)	Boring diameter (mm)
SA-1	11.5	7.5	4.0	10.5	105
SA-2	11.5	6.5	5.0	10.5	105

Fig. 11 Arrangement of FBG sensors in each anchor: (a) SA-1, (b) SA-2

first FBG sensors of each anchor during the introducing stage of the prestress force. Each FBG sensors have a different initial reflection wavelength and different wavelength shifts are clearly shown with respect to time during prestressing. Prestress force P_{FBG} estimated using the wavelength shift data measured from the first FBG sensor with Eq. (6) is compared with prestress force $P_{load\ cell}$ measured from the conventional load cell shown in Fig. 14. From the figure, one can find that prestress force determined with the strain measured from FBG sensors matches well with the introduced prestress force precisely within the design prestress force.
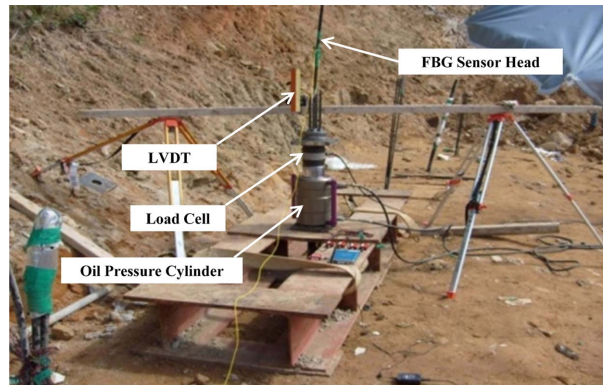
Fig. 12 Pullout test setup for monitoring of prestress force and load transfer of proto-type anchor
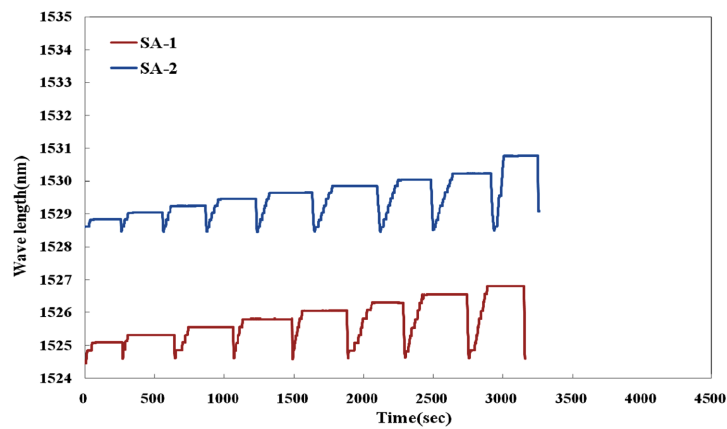

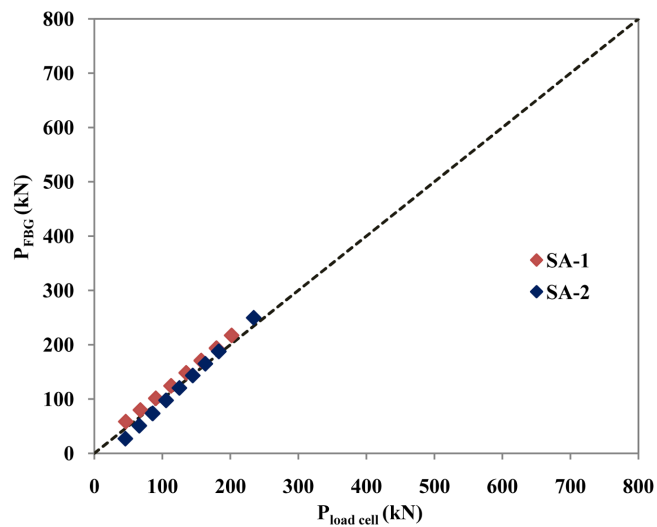Fig. 13 Wavelength shift data measured from the first FBG sensors of each anchor

Fig. 14. Comparison of prestress force estimated from the measurement of wavelength shift using first FBG sensor in smart tendon with that measured from load cell within the design capacity

$$\boldsymbol{P}_{\mathbf{FBG}} = n \times A_t \times E_t \times \varepsilon_{FBG} \tag{6}$$

where $\boldsymbol{P}_{\mathbf{FBG}}$ is a pressing force determined based on the strain measured from the FBG, n is number of tendon in ground anchor, E_t is a Young's modulus of the tendon (= 200 GPa), A_t is an effective cross-sectional area of the tendon (= 140 mm^2), ε_{FBG} is strain measured from the first FBG sensor located at the free part.

　　Load transfer was also measured during prestressing with 4 FBG sensors distributed at the fixed part as shown in Fig. 11. Figs. 15 and 16 clearly show the distribution of the introduced prestress
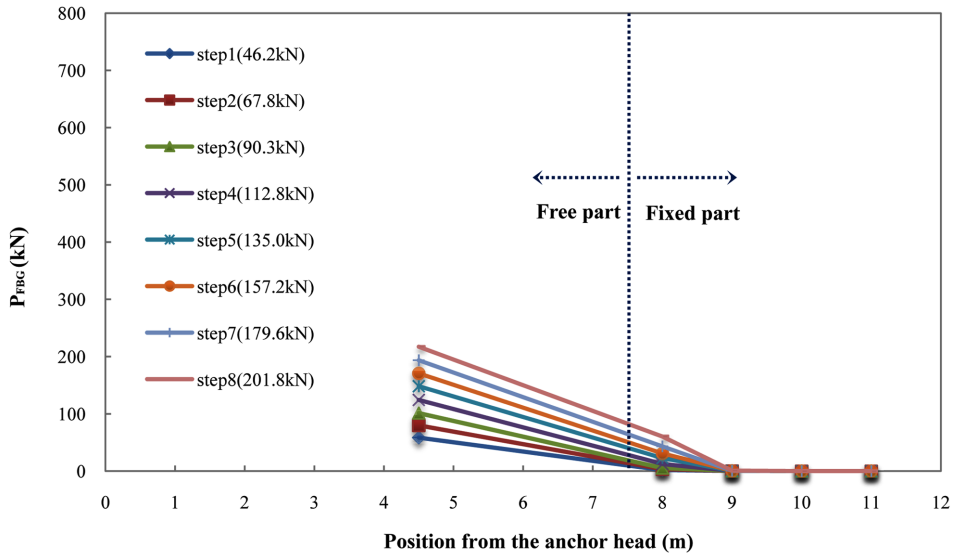

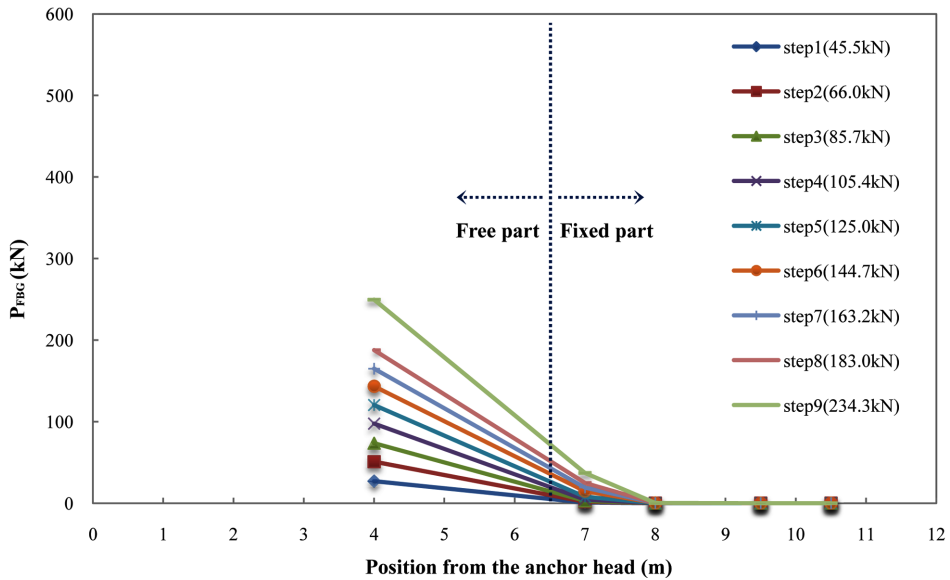Fig. 15 Load transfer measured from FBGs at fixed part of anchor SA-1

Fig. 16 Load transfer measured from FBGs at fixed part of anchor SA-2

force and transfer of the prestress force from the initial part of the fixed part to the direction of end of the fixed part. As shown in Figs. 15 and 16, the introduced prestress was finally transferred up to 1.5 m for the SA-1 and SA-2, respectively. From the test results, we may expect that the proposed smart tendon can be used to improve the design practice through determining the economic fixed length by practically measuring the load transfer depth.

4. Conclusions

A novel technique for measuring the tensile force of a 7-wire steel strand, named smart tendon, is applied to monitor the prestress force and load transfer of ground anchor. The optical sensor is encapsulated in the central king wire of the 7-wire strand by replacing the king wire with a steel tube in which the FBG sensors scribed in the optical fiber are tightly coupled by means of injected water-like epoxy resin having a low viscosity.

The idea is first verified by tensile tests for 1.0 m long specimens, which showed excellent agreement with the measurement of strain gauge attached outside of the tendon. The technique is then applied to measure the load transfer mechanism of the model anchor at the laboratory test. The prestress force transfer phenomenon was clearly shown with increasing applied load. Finally, it is applied to an 11.5 m long prototype ground anchor for monitoring both the prestress force and the load transfer phenomenon from the introducing process of the prestress to the long-period. With the FBG sensor installed at the free part and fixed part, the instantaneous monitoring of the prestress force and load transfer phenomenon was successfully monitored.

Based on these test results, the proposed smart tendon is not only expected to be an alternative monitoring tool for measuring prestress force from the introducing stage to the long-term period for health monitoring of the ground anchor but also can be used to improve design practice through determining the economic fixed length by practically measuring the load transfer depth.

Acknowledgements

References

Aalami, B.O. (1998), "Time-dependent analysis of post-tensioned concrete structures", *Prog. Struct. Eng. Mat.*, **1**(4), 384-391.

Aydan, O., Ebisu, S. and Komura, S. (1993), "Pull-out tests of rock anchors and their failure modes", *Proceedings of the Int. Symp. On Assessment and Prevention of Failure Phenomena in Rock Engineering*, Istanbul, Turkey.

Aydan, O., Komura, S., Ebisu, S. and Kawamato, T. (1995), "A unified design method for anchor foundations of super-high pylons", *Proceedings of the Int. Symp. Workshop on Rock Foundation*, Tokyo, Japan.

Brady, K. and Bush, D. (2001), "The performance of load cells used for ground anchors", *Proceedings of the 15th ICSMGE*, Istanbul, Turkey.

Bruce, S.M., McCarten, P.S., Freitag, S.A. and Hasson, L.M. (2008), "Deterioration of prestressed concrete bridge beams", *Research Report 337*, Land Transport, New Zealand.

Calvert, S. and Mooney, J. (2004), "Bridge structural health monitoring system using fiber grating sensors: development and preparation for a permanent installation", *Proceedings of the SPIE.*

Georgiades, A.V., Saha, G.C., Kalamkarov, A.L., Rokkam, S.K., Newhook, J.P. and Challagulla, K.S. (2005), "Embedded smart GFRP reinforcements for monitoring reinforced concrete flexural components", *Smart Struct. Syst.,* **1**(4), 369-384.

Farmer, I.W. (1975), "Stress distribution along a resin grouted rock anchor", *Int. J. Rock Mech. Min. Sci. Geomech. Abstr.*, **12**(11), 347-351.

Fricker, S. and Vogel, T. (2006), "Detecting wire breaks in a prestressed concrete road bridge with continuous acoustic monitoring", *Proceedings of the 3rd Int. Conf. on Bridge Maintenance, Safety and Management*, Porto, Portugal.

Inaudi, D. (2000), "Application of civil structural monitoring in Europe using fiber optic sensors", *Prog. Struct. Eng. Mat.*, **2**(3), 351-358.

Kesavan, K., Ravisankar, K., Parivallal, S. and Sreeshylam, P. (2005), "Applications of fiber optic sensors for structural health monitoring", *Smart Struct. Syst.*, **1**(4), 355-368.

Kim, J.T., Park, J.H., Hong, D.S., Cho, H.M., Na, W.B. and Yi, J.H. (2009), "Vibration and impedance monitoring for prestress-loss prediction in PSC girder bridges", *Smart Struct. Syst.*, **5**(1), 81-94.

Kim, Y.S., Kim, J.M., Suh, D.N., Sung, H.J. and Lee, S.L. (2009), "Measurement of load transfer between anchor and grout using optical FBG sensors embedded smart tendon", *Safety, Reliability and Risk of Struct., Infrastructures and Engineering Systems*, Fruta, (Eds. Frangopol and Shinozuka), Taylor & Francis Group, London.

Lakshmanan, N., Saibabu, S., Murthy, A.R.C., Ganapathi, S.C. and Jayaraman, R. (2009), "Experimental, numerical and analytical studies on a novel external prestressing technique for concrete structural components", Comput. *Concrete.*, **6**(1), 41-57.

Lau, K.T. (2003), "Fibre-optic sensors and smart composites for concrete applications", *Mag. Concrete. Res.*, **55**(1), 19-34.

Li, E., Xi, J., Chicharo, J., Liu, T., Li, X., Jiang, J., Li, L., Wang, Y. and Zhang, Y. (2005), "The experimental evaluation of FBG sensor for strain measurement of prestressed steel strand", *Proceedings of the SPIE,* 5649.

Meissner, J., Nowak, W., Slowik, V. and Klink, T. (1997), "Strain monitoring at a prestressed concrete bridge", *Proceedings of the Optical Fiber Sensors*, Williamsburg, Virginia, October.

Moerman, W., Taerwe, L., Waele, W. D, Degrieck, J. and Himpe, J. (2005), "Measuring ground anchor forces of a quay wall with bragg sensors", *J. Struct. Eng.-ASCE*, **131**(2), 322-328.

Nellen, P.M., Anderegg, P., Bronnimann, R., Meier, U. and Sennhauser, U. (1999a), "Fiber optical Bragg grating embedded in CFRP wires", *Proceedings of the SPIE,* 3870.

Nellen, P.M., Bronnimann, R., Frank, A., Mauron, P. and Sennhauser, U. (1999b), "Structurally embedded fiber Bragg gratings: civil engineering application*", Proceedings of the SPIE,* 3860.

Onyemelukwe, O. and Kunnath, S. (1997), "Field measurement and evaluation of time-dependent losses in prestressed concrete bridges", *Research Report.*

Othonos, A. and Kalli, K. (1999), *Fiber Bragg Gratings,* Artech House, London.

Ren, L., Li, N.H., Sun, L. and Li, D.S. (2005), "Development of tube-packaged FBG strain sensor and application in the vibration experiment of submarine pipeline model", *Proceedings of the SPIE,* 5770.

Samwoo Geotechnical Co. Ltd, http://www.swanchor.com

Shenoy, C.V. and Frantz, G.C. (1991), "Structural tests of 27-year-old prestressed concrete bridge beams", *PCI J.*, 80-90.

Talebinejad, I., Fischer, C. and Ansari, F. (2009), "Serially multiplexed FBG accelerometer for structural health monitoring of bridges", *Smart Struct. Syst.*, **5**(4), 345-355.

Udd, E. (1995), "*Fiber Optic Smart Structure*", John Wiley & Sons, Inc.

Vurpillot, S., Inaudi, D. and Ducret, J.M. (1996), "Bridge monitoring by fiber optic deformation sensors: design, emplacement and results", *Proceedings of the SPIE, Smart Struct. Mat.,* San Diego.

Wang, M. L. (2008), "Long term health monitoring of post-tensioning box girder bridges", *Smart Struct. Syst.,* **4**(6), 711-726.

Won, S.Y., Cho, N.J. and Hwang, S.I. (2001), "Stress Distribution of Ground Rock Anchors", *J. KSCE*, **21**(3),

257-266.

Youn, S.G. and Kim, E.K. (2006), "Deterioration of bonded post-tensioned concrete bridges and research topics on the strength evaluation in ISARC", *Proceedings of the JSCE-KSCE Joint Sem. on Maint. & Mana. Strategy of Infrastruct. in Japan and Korea*, Kusatsu, Shiga, Japan, September

Zhou. Z., Thomas W.G., Luke Hsu and Ou, J.P. (2003), "Techniques of advanced FBG sensors: fabrication, demodulation, encapsulation and their application in the structural health monitoring of bridges", *Pacific Sci. Review*, **5**, 116-121.